

NOAA Technical Report NESDIS 34



# Balloon-Based Infrared Solar Occultation Measurements of Stratospheric O<sub>3</sub>, H<sub>2</sub>O, HNO<sub>3</sub>, and CF<sub>2</sub>C1<sub>2</sub>

Washington, D.C.  
September 1987

**DUPLICATE  
WITHDRAWN**

**U.S. DEPARTMENT OF COMMERCE**  
**National Oceanic and Atmospheric Administration**  
National Environmental Satellite, Data, and Information Service

NOAA TECHNICAL REPORTS  
National Environmental Satellite, Data, and Information Service

The National Environmental Satellite, Data, and Information Service (NESDIS) manages the Nation's civil Earth-observing satellite systems, as well as global national data bases for meteorology, oceanography, geophysics, and solar-terrestrial sciences. From these sources, it develops and disseminates environmental data and information products critical to the protection of life and property, national defense, the national economy, energy development and distribution, global food supplies, and the development of natural resources.

Publication in the NOAA Technical Report series does not preclude later publication in scientific journals in expanded or modified form. The NESDIS series of NOAA Technical Reports is a continuation of the former NESS and EDIS series of NOAA Technical Reports and the NESC and EDS series of Environmental Science Services Administration (ESSA) Technical Reports.

These reports are available from the National Technical Information Service (NTIS), U.S. Department of Commerce, Sills Bldg., 5285 Port Royal Road, Springfield, VA 22161 (prices on request for paper copies or microfiche, please refer to PB number when ordering) or by contacting Nancy Everson, NOAA/NESDIS, 5200 Auth Road, Washington, DC 20233 (when extra copies are available). A partial listing of more recent reports appear below:

NESDIS SERIES

- NESDIS 1 Satellite Observations on Variations in Southern Hemisphere Snow Cover. Kenneth F. Dewey and Richard Heim, Jr., June 1983. (PB83 252908)
- NESDIS 2 NODC 1 An Environmental Guide to Ocean Thermal Energy Conversion (OTEC) Operations in the Gulf of Mexico. National Oceanographic Data Center, June 1983. (PB84 115146)
- NESDIS 3 Determination of the Planetary Radiation Budget from TIROS-N Satellites. Arnold Gruber, Irwin Ruff and Charles Earnest, August 1983. (PB84 100916)
- NESDIS 4 Some Applications of Satellite Radiation Observations to Climate Studies. T.S. Chen, George Ohring and Haim Ganot, September 1983. (PB84 108109)
- NESDIS 5 A Statistical Technique for Forecasting Severe Weather from Vertical Soundings by Satellite and Radiosonde. David L. Keller and William L. Smith, June 1983. (PB84 114099)
- NESDIS 6 Spatial and Temporal Distribution of Northern Hemisphere Snow Cover. Burt J. Morse and Chester F. Ropelewski (NWS), October 1983. (PB84 118348)
- NESDIS 7 Fire Detection Using the NOAA--Series Satellites. Michael Matson, Stanley R. Schneider, Billie Aldridge and Barry Satchwell (NWS), January 1984. (PB84 176890)
- NESDIS 8 Monitoring of Long Waves in the Eastern Equatorial Pacific 1981-83 Using Satellite Multi-Channel Sea Surface Temperature Charts. Richard Legeckis and William Pichel, April 1984. (PB84 190487)
- NESDIS 9 The NESDIS-SEL Lear Aircraft Instruments and Data Recording System. Gilbert R. Smith, Kenneth O. Hayes, John S. Knoll and Robert S. Koyanagi, June 1984. (PB84 219674)
- NESDIS 10 Atlas of Reflectance Patterns for Uniform Earth and Cloud Surfaces (NIMBUS-7 ERB--61 Days). V.R. Taylor and L.L. Stowe, July 1984. (PB85 12440)
- NESDIS 11 Tropical Cyclone Intensity Analysis Using Satellite Data. Vernon F. Dvorak, September 1984. (PB85 112951)
- NESDIS 12 Utilization of the Polar Platform of NASA's Space Station Program for Operational Earth Observations. John H. McElroy and Stanley R. Schneider, September 1984. (PB85 1525027AS)

NOAA Technical Report NESDIS 34



# Balloon-Based Infrared Solar Occultation Measurements of Stratospheric O<sub>3</sub>, H<sub>2</sub>O, HNO<sub>3</sub>, and CF<sub>2</sub>C1<sub>2</sub>

Michael P. Weinreb

I-Lok Chang  
The American University  
Washington, D.C.

Washington, D.C.  
September 1987

**U.S. DEPARTMENT OF COMMERCE**  
Clarence J. Brown, Acting Secretary

**National Oceanic and Atmospheric Administration**  
J. Curtis Mack II, Acting Under Secretary

**National Environmental Satellite, Data, and Information Service**  
Thomas N. Pyke, Jr., Assistant Administrator

## CONTENTS

Abstract . . . . .	1
1. Introduction . . . . .	1
2. Description of the Experiment . . . . .	3
3. Data Reduction . . . . .	5
3.1. Conversion of Raw Data to Transmittances . . . . .	5
3.2. Retrieval Procedure . . . . .	6
3.3. Error Analysis . . . . .	8
4. Results and Discussion . . . . .	9
4.1. Ozone . . . . .	9
4.2. Water Vapor . . . . .	9
4.3. Nitric Acid . . . . .	10
4.4. CFC-12 . . . . .	11
5. Conclusion . . . . .	12
Acknowledgments . . . . .	13
References . . . . .	14

## TABLES

1. Spectral Intervals (Channels) for Balloon Spectrometer . . . . .	3
2. Measurement Timetable . . . . .	5

## FIGURES

1. Solar Occultation Geometry . . . . .	18
2. Measured Transmittances--Channels 1 and 2 . . . . .	19
3. Measured Transmittances--Channels 4, 5, and 6 . . . . .	20
4. First-Guess Mixing Ratio Profiles--Nitric Acid and CFC-12 . . . . .	21

5.	Estimated Transmittance Errors--Channel 5 . . . . .	22
6.	Retrieved Ozone Profile and Concurrent ECC Measurements . .	23
7.	Retrieved Water Vapor Profile and Concurrent Frost-Point Hygrometer Measurements . . . . .	24
8.	Retrieved Nitric Acid Profile and Previous Measurements . .	25
9.	Retrieved Nitric Acid Profile and 1979 Measurements .. . . .	26
10.	Retrieved CFC-12 Profile and Envelope of Prior Measurements	27

Balloon-Based Infrared Solar Occultation Measurements  
of Stratospheric O<sub>3</sub>, H<sub>2</sub>O, HNO<sub>3</sub>, and CF<sub>2</sub>Cl<sub>2</sub>

Michael P. Weinreb

National Oceanic and Atmospheric Administration  
National Environmental Satellite, Data, and Information Service  
Washington D. C.

I-Lok Chang

The American University  
Washington, D. C.

ABSTRACT. In July 1985 we performed an infrared solar occultation experiment with a balloon-borne, non-scanning, multi-detector grating spectrometer. From the data we retrieved simultaneous mixing ratio profiles of ozone, water vapor, nitric acid, and CFC-12 between 12 and 35 km. The retrieved ozone and water vapor profiles were compared with concurrent in-situ measurements with electrochemical concentration cells (ECC's) and frost-point hygrometers, respectively. The retrieved ozone profile was in good agreement with the correlative data. The retrieved values of water vapor mixing ratio, while close in magnitude to the correlative measurements, differed in their altitude dependence. Although we had no concurrent in-situ data for nitric acid and CFC-12, the retrieved profiles were consistent with measurements in the literature.

## 1. INTRODUCTION

We have conducted a series of balloon-based experiments using infrared solar occultation, implemented with a multi-detector, non-scanning spectrometer, to infer the mixing ratios of trace gases in the stratosphere. The purpose of these experiments was to assess how feasible the technique is for long-term monitoring of the stratosphere from satellites. Stationed at an altitude of approximately 40 km, the spectrometer collected solar radiation transmitted by the atmosphere's limb for several hours before and during sunset. Observations were made simultaneously in the absorption bands of ozone, water vapor, nitric acid, and CF<sub>2</sub>Cl<sub>2</sub> (CFC-12). Mixing ratio profiles were retrieved mathematically from the data.

Occultation measurements have been made with satellite-borne infrared spectrometers in the Stratospheric Aerosol and Gas Experiment (SAGE) and the Stratospheric Aerosol Measurement II (SAM II) [McCormick et al., 1979]. Observing the stratosphere at wavelengths between 0.38 and 1  $\mu$ m, they have produced extensive measurements of aerosols, ozone, and nitrogen dioxide [e.g., Kent and McCormick, 1984;

McCormick et al., 1984]. Our experiments were aimed at extending the SAGE and SAM II technique to longer wavelengths (6-12  $\mu\text{m}$ ) and to a larger group of constituents.

A related infrared technique, limb emission, has been applied with the Limb Radiance Inversion Radiometer (LRIR) [Gille et al., 1980] on the Nimbus-6 satellite and by the Limb Infrared Monitor of the Stratosphere (LIMS) [Gille and Russell, 1984] and the Stratospheric and Mesospheric Sounder (SAMS) [Rodgers et al., 1984] on the Nimbus-7 satellite to measure mixing ratios of stratospheric constituents. We chose instead to study solar occultation, because it has several advantages over limb emission, which derive from its use of the sun as the radiation source. The high intensity of the incoming radiation allows the use of unsophisticated detector technology and minimal cooling of the instrument. Since the instrument's spectral intervals can be relatively narrow, they can usually be located to minimize interfering absorption by gases other than than one being sensed. With occultation, atmospheric emission is negligible in comparison to the solar signal. That simplifies the mathematics of the retrieval and minimizes its sensitivity to the vertical temperature profile. On the other hand, the principal disadvantage of occultation is that, since it can be carried out only at sunrise or sunset, it gives less geographical and temporal coverage than does limb emission.

Numerous measurements of stratospheric constituents have been made previously from balloons and aircraft with the infrared solar occultation technique (e.g., Murcray et al. [1967], Murcray et al. [1979], Girard et al. [1977], Farmer et al. [1980], and Fischer et al. [1985]). The experiment reported in this paper is different because its purpose is different. First, our instrument--the non-scanning, multi-detector spectrometer--was chosen because it has capabilities required in long-term satellite monitoring, such as simplicity, reliability, long life, and low data rates. These requirements eliminated from consideration more sophisticated instrumentation such as interferometers or pressure modulated radiometers. Also, the spectrometer offers a spectral purity difficult to obtain with filter radiometers. Second, the experiment was designed to simulate a satellite measurement as much as possible. For example, observations were made only when the balloon was at float, not during ascent or descent. Third, since we want to estimate the accuracy of the occultation measurements, we arranged to have in situ soundings of ozone and water vapor made at approximately the same time and place as the occultation experiment. Although accuracies cannot be determined precisely, comparisons with in situ data are a valuable indicator.

We have already described the technique and the results from our first flight, which took place at Palestine, Texas, on June 21, 1982 [Weinreb et al., 1984]. That flight yielded measurements of mixing ratio profiles of ozone, water vapor, and nitric acid between 25 and 39 km. A flaw in the sun-tracking system prevented acquisition of data for altitudes below 25 km. Also, the correlative in-situ measurements were only partially successful, yielding ozone data with considerable scatter and no data on water vapor. A second balloon-flight experiment was carried out in April 1983. An

unexpected feature, possibly absorption by atmospheric aerosols, appeared in the occultation measurements, overlapping the absorption by the gases of interest. Without additional spectral information, perhaps obtainable from spectral scanning or from measurements in window channels located in the spectrum where there is no gaseous absorption, we could not identify the cause of the feature or unambiguously remove its effects from the measurements. Furthermore, we could not entirely rule out the instrument as the cause. Therefore, the results from the second flight are not being reported.

This paper documents the results from the third flight, which took place at Palestine on July 5, 1985. In that experiment we did not detect any unexpected absorption. A redesigned sun-tracking system enabled us to acquire clean data down to 12 km, increasing the extent of the retrieved profiles and permitting us to detect CFC-12 for the first time in our experiments. In addition, the correlative data, collected for both water vapor and ozone, were of higher quality than they had been in the previous experiments.

## 2. DESCRIPTION OF THE EXPERIMENT

The geometry of the experiment is illustrated in Figure 1. Held at float altitude by the balloon, the instrument measures the solar intensity as a function of solar zenith angle between  $90^\circ$  and roughly  $95^\circ$ . As is described in Section 3, the data, converted to the form of limb transmittances vs tangent height, are processed to yield profiles of volume mixing ratios vs height.

The instrument has been described previously [Weinreb et al., 1984]. In brief, it is a multi-detector grating spectrometer that detects radiation continuously in eight discrete infrared spectral intervals (channels). Six of the channels, located in the absorption bands of  $\text{HNO}_3$ ,  $\text{CF}_2\text{Cl}_2$ ,  $\text{O}_3$ , and  $\text{H}_2\text{O}$ , are described in Table 1. (Data in the other two channels were not used, for reasons discussed in Weinreb et al. [1984]). The detectors are uncooled thermistors. More sensitive detectors are unnecessary because the sun is such an intense source of radiation.

TABLE 1. Spectral Intervals (Channels) for Balloon Spectrometer

Channel	Central Wavenumber ( $\text{cm}^{-1}$ )	Half-Power Bandwidth ( $\text{cm}^{-1}$ )	Species
1	886	5	Nitric acid
2	930	4	CFC-12
3	980	6	Ozone, low altitude
4	998	3	Ozone, high altitude
5	1507.0	3	Water vapor, high altitude
6	1528.5	4.5	Water vapor, low altitude

Radiation is focussed onto the spectrometer by an f/4.5 Cassegrain telescope with a focal length of 600 mm. The angular field of view is a rectangle 4.5 arc min in azimuth and 8.3 arc min in elevation. (For comparison, note that the sun's diameter is approximately 32 arc min.) It subtends a linear field of view of approximately 1.8 km at a tangent height of 12 km and 0.6 km at a tangent height of 35 km. However, along any ray below the horizontal, absorption by the atmosphere occurs in a layer whose vertical extent is larger than the instrument's field of view. The vertical extent of the absorbing layer, also referred to as the width of the weighting function, is approximately 3 km for most tangent heights. It is determined by both the field of view and the absorption properties of the atmosphere. In this experiment the latter is the more important, since even with an infinitesimal field of view, the weighting function is close to 3 km wide for most tangent heights.

The sun-tracking system was redesigned for this flight. In the first two flights the entire instrument had been pivoted in azimuth and elevation on two sets of gimbels. For this flight the University of Denver supplied a new system like the one described in Murcray et al. [1967]. Our instrument, now fixed to the gondola, could no longer rotate. Instead, the solar radiation was directed into the instrument by a mirror that rotated in azimuth and elevation, driven by the signals from two pairs of detectors, one pair for azimuth, the other for elevation. The position of the field of view on the face of the sun was monitored by two additional pairs of detectors, located inside the telescope. For the data to be valid, the field of view must remain on the non-limb-darkened portion of the sun. During most of the observing period, the field of view oscillated about a point slightly below the center of the sun with an amplitude of approximately 1.5 arc min and a period of 25 sec. Near the end of the experiment, as the sun approached the horizon, the field of view began to drift and the amplitude of the oscillations to increase. However, good data were acquired down to a tangent height of 12 km. This is a considerable improvement over the earlier experiments, in which no data were acquired below 23 km.

For this flight the instrument was modified in one other way: the baffling in the telescope was increased to reduce scattered radiation in the instrument. Although scattered radiation had been negligible in tests in the laboratory before the flight, the appearance of an unexplained feature in the data of the second flight motivated us to take whatever steps we could to eliminate instrument effects.

The third flight experiment took place at Palestine, TX, on July 5, 1985. The balloon reached a float altitude of 39 km in the late afternoon and remained within 1 km of that altitude until the experiment was terminated after sunset. Generally, the instrument operated reliably and provided data with low noise. However, there were two problems: First, the electronic gain for channel 3 was unstable. As a result, only the data in channel 4 were usable for sounding ozone. Second, transmission of data from the gondola to the ground was temporarily interrupted during the observations between the tangent heights of 38 and 36 km. This degraded the expected accuracy of the retrievals above 30 km, as we describe later in this paper.

As we mentioned previously, a series of in-situ soundings of ozone and water-vapor mixing ratio profiles were also made at Palestine within a few hours of the occultation experiment. They were carried out by a group from the NOAA/Environmental Research Laboratories under the direction of S. J. Oltmans. Ozone was sounded with balloon-borne model-4A electrochemical concentration cells (ECC's) [Komyhr, 1969]. Each measurement was normalized to the total ozone amount measured at Palestine on the same day with a Dobson spectrophotometer. Water vapor was sounded with frost-point hygrometers [Mastenbrook and Oltmans, 1983]. An approximate timetable of all the soundings, both occultation and in situ, is shown in Table 2. The two types of measurements ranged from nearly coincident to nearly 12 hours apart. There were also spatial differences, because at sunset an occultation experiment sounds the atmosphere several hundred kilometers west of the observing instrument. Consequently, if there is variability in the atmosphere over these times and distances, the occultation and in-situ measurements will differ. Along with possible errors in the in-situ data themselves, the lack of temporal and spatial coincidence makes it difficult to infer accuracy unambiguously from a single measurement. Nevertheless, comparisons with in-situ data are valuable indicators of accuracy.

TABLE 2. Measurement Timetable

Date	Time (GMT)	Event
7/5/85	2100	Launch of hygrometer #1
7/6/85	0000	Launch of hygrometer #2
7/6/85	0200	IR occultation observations
7/6/85	0400	Launch of ECC #1
7/6/85	1200	Launch of ECC #2

### 3. DATA REDUCTION

#### 3.1 Conversion of Raw Data to Transmittances

The flight data were received as a stream of detector output, in volts, versus time. However, the retrieval algorithms require the data to be in the form of transmittance versus tangent height. The data were converted to this form by techniques described in detail in Chang and Weinreb [1987] and summarized here.

Times of observation were converted to solar zenith angles by calculations based on the ephemeris of the sun. Then the solar zenith angles were transformed to tangent heights with an atmospheric ray trace, which included effects of refraction. The calculations also accounted for the small oscillation of the instrument's field of view on the face of the sun and for small changes in the altitude of the balloon, monitored by on-board pressure gauges.

We transformed the voltages measured during the occultation period to transmittances by dividing them by the 100% signals, i.e., the signals that would be measured in the absence of any atmosphere. In channels 1, 2, and 6 the atmospheric absorption is so weak that the signals measured before sunset, when the solar zenith angle is relatively small, are essentially the 100% signals. However, in the other channels atmospheric absorption is stronger, and direct measurement of the 100% signal is impossible. In those channels we inferred the 100% signals by extrapolating to zero airmass the signals measured before the solar zenith angle reached  $90^\circ$ .

Previously we had mentioned that the data for the tangent heights between 38 and 36 km were missing. We inferred transmittance values for these tangent heights by interpolating with cubic Hermite polynomials between the measured values on either side of the gap. The errors in this procedure may be a significant fraction of the signal (i.e., the measured absorption), since atmospheric absorption is small at these levels. Therefore, we did not have much confidence in the retrieved profiles between 38 and 36 km. However, the interpolated transmittances can be used in the retrievals at lower levels, where atmospheric absorption is stronger. The influence of these errors on the retrieved profiles decreases with decreasing altitude, and below 30 km their influence becomes negligible.

The transmittance profiles (i.e., transmittance vs tangent height) are displayed in Figures 2-3. Henceforth we will refer to these transmittances as "measured" transmittances. They are the data from which the mixing ratio profiles are retrieved. The transmittances are specified for each integral value of the tangent height. Each point represents data averaged over 8.5 seconds. In 8.5 seconds the sun descends approximately 2.2 arc minutes. That is one quarter of the vertical extent of the instrument's field of view, so the averaging causes practically no degradation of the vertical resolution. Transmittance data acquired before the solar zenith angle reached  $90^\circ$ , which were also used in the retrievals, are not shown.

### 3.2 Retrieval Procedure

To solve for mixing ratio profiles, we invert a system of equations that state the equality between the measured transmittances and a set of transmittances calculated from the atmospheric conditions, including the mixing ratios; i.e.,

$$t_i(q_1, \dots, q_i, \dots, q_N) + e_i = T_i \quad i=1, 2, \dots, M$$

where  $t$  is the calculated transmittance,  $T$  the measured transmittance,  $q$  the mixing ratio, and  $e$  an error term, primarily errors of measurement and quadrature. The subscript  $i$  refers to the  $i$ th tangent height or atmospheric level. The constants  $M$  and  $N$  are the number of tangent heights for which measurements are used and the number of levels at which mixing ratios are retrieved, respectively. Normally this system of equations corresponded only to measurements at solar

zenith angles greater than  $90^{\circ}$ . However, for the ozone and water vapor retrievals, we also used a few measurements made at solar zenith angles less than  $90^{\circ}$ . These were added to prevent the profile above the balloon from being grossly in error; otherwise large errors there could propagate down into the retrieved profile below the balloon.

We solve the system by iterative application of the Levenberg-Marquardt algorithm, a matrix inverse method, that is described in Weinreb et al. [1984] and Chang and Weinreb [1987]. Ozone profiles were retrieved from the measurements in channel 4, and the water vapor profiles from the data in channels 5 and 6. Because the data between 36 and 38 km were missing, the retrieved profiles are only shown at levels below 36 km. The nitric acid and CFC-12 profiles were retrieved simultaneously from data in channels 1 and 2, since absorption by both species is present in both channels.

The iterations begin with a first-guess profile. For ozone the first guess is the mid-latitude model of Krueger and Minzner [1976]. For water vapor it is 5 ppmv at all altitudes. The nitric acid and CFC-12 first guesses were provided by the LIMS Experiment Team [W. Planet, unpublished data, 1977] and are plotted in Fig. 4. Sensitivity of the retrievals to the first guess was discussed for ozone in Weinreb et al. [1984]. In essence, the sensitivity varies inversely with the strength of the atmospheric signal.

Computations of atmospheric transmittances are also required. For nitric acid we used a band model formulated by Goldman et al. [1981]. For CFC-12 we used a similar band model from Goldman et al. [1976] modified to include the temperature dependence of Harward [1978] and the band strength of Kagann et al. [1983]. For water vapor and ozone we used an efficient approximation [Weinreb et al., 1984] fitted to line-by-line calculations made with FASCODE [Smith et al., 1978] and based on molecular line data from the 1982 AFGL tape [Rothman et al., 1983]. The effects of interfering spectra of other gases are small but not completely negligible in the spectral intervals of this instrument. In channel 1 (nitric acid) the calculations below 22 km included a small component from CFC-12, and in channel 2 (CFC-12) they included small components from nitric acid and carbon dioxide. (Transmittances of carbon dioxide were calculated once and for all with the line-by-line code.) In channels 5 and 6 (water vapor) the transmittance calculations included the effect of collision-induced absorption by oxygen [Shapiro and Gush, 1966], which is very important for tangent heights below 25 km. The oxygen calculations were based on coefficients from Shapiro and Gush [1966], which we verified by using them to reproduce measurements of atmospheric oxygen absorption presented in Rinsland et al. [1982].

Knowledge of the atmospheric profiles of temperature and height vs pressure is also needed in the data reduction, both for determining the altitude of the balloon from the on-board measurements of atmospheric pressure and for the transmittance calculations. Those profiles were acquired from the upper-air analyses of the National Meteorological Center's Climate Analysis Center.

### 3.3 Error Analysis

Errors in the retrieved profiles can be caused by errors both in the measurements and in the retrieval procedures. To quantify the relative importance of the various error sources, we used simulations to compute profiles of transmittance errors that would result from errors one might reasonably expect to occur in the experiment. We found that the measured transmittances are most sensitive to errors in specifying the altitude of the balloon and the zenith angle of the line of sight, and in the calibration equation that converts the raw data to transmittances. Similar errors will also affect satellite occultation measurements. In this experiment, we estimated the maximum uncertainty to be 0.4 km in the balloon altitude and 2 arc min in the zenith angle. In the calibration equation, which relates output volts to measured transmittance, the systematic errors were estimated to be between 0.005 and 0.01 in offset and between 0.5% and 1% in gain, depending upon the channel. Errors in the transmittances caused by the interpolation between 38 and 36 km were added to the calibration error. Other systematic errors (see, e.g., Shaffer et al. [1984]) and the random errors of measurement (noise) were found to be less important at most altitudes than the systematic errors from the sources just discussed.

The major source of error in the retrieval algorithm is the calculation of transmittances. This will also be an important source of error in a satellite measurement. These errors arise from uncertainties in the spectral response functions and the spectroscopic line parameters, from limitations of our models for approximating the line-by-line calculations, and, to a lesser extent, from uncertainties in the atmospheric temperature profile. In addition, the transmittances calculated for CFC-12, nitric acid, and the pressure-induced absorption by molecular oxygen could be significantly in error by several percent (in transmittance), since they are based on empirical models instead of line-by-line calculations.

Figure 5 presents an example of transmittance error profiles for the most important sources. These data are for channel 5. In the figure, "pointing error" refers to errors in the zenith angle of the line of sight, and "calculation errors" to errors in the transmittance calculations.

To estimate the uncertainties in the retrieved mixing ratios, we performed the retrievals both before and after perturbing the measured transmittance profile by an error profile whose elements are rss's (roots of the sums of squares) of the transmittance errors from each source mentioned above. (Note that this procedure lumps the errors in the transmittance calculations with those of the measured transmittances.) The difference between the two retrieved mixing ratio profiles was interpreted as the profile of uncertainties.

## 4. RESULTS AND DISCUSSION

### 4.1 Ozone

Figure 6 shows the retrieved ozone profile, accompanied by two profiles measured with concurrent ECC's. The uncertainties in the retrieved profiles are indicated by the error bars. (Half the length of the bar is the computed uncertainty.) Above 25 km the uncertainties are approximately 10% of the retrieved values. Between 16 and 25 km they range between 5 and 20%. Below 16 km, where the signal is relatively insensitive to the mixing ratio, they exceed 100% (not shown). The ECC data exhibit little scatter below 33 km, which is evidence for the precision of the ECC's and constancy of ozone over eight hours. The ECCs' precision is estimated by Hilsenrath et al. [1986] to be about 3% between 20 and 33 km and 7% elsewhere. Above 30 km the ECC may exhibit a bias towards low values that worsens with altitude.

At almost all levels the retrieved profile and the ECC soundings agree when the uncertainties of each are taken into account. The agreement above 25 km is very good--comparable to the precision of the ECC's. Between 30 and 34 km the ECC data show no bias relative to the retrieved profile. This is consistent with the results of mid-latitude comparisons between LIMS and ECC profiles, which give a mean LIMS-minus-ECC bias of less than 4% above 31 km (10 mb) [Remsburg et al., 1984]. At most levels below 25 km the differences between the retrieved profile and the ECC's are less than 10% and are smaller than the combined uncertainties in the two techniques. The larger discrepancies at 22 km, 19 km, and near 15 km are unexplained.

### 4.2 Water Vapor

Figure 7 shows the retrieved water vapor profile, along with the upper segments of the profiles measured concurrently with the two frost-point hygrometers. The large uncertainties in the retrieved profile at 18 km and below are associated with the rapid increase in the measured transmittances with tangent height in channels 5 and 6 (see Figure 3). In consequence, pointing errors and uncertainties in the balloon altitude translate into large uncertainties in the measured transmittances. Above 18 km the uncertainties in the retrieved profile range from 10 to 30%. The uncertainties associated with the hygrometer data are estimated to be no larger than 17% [Mastenbrook and Oltmans, 1983], which is roughly equivalent to 1 ppmv in the profiles in the figure.

Above 17 km the hygrometer data exhibit remarkably little scatter. However, near the tropopause (15 km) they show high-frequency variations in the vertical on a scale of one kilometer or less, and the measurements by the two hygrometers differ considerably. These are probably real temporal and spatial variations in the atmosphere. The occultation measurements cannot resolve such fine vertical structure. As we mentioned previously, the signal (absorption) for a ray with a 15 km tangent height originates in a layer with a vertical extent of approximately 3 km.

The retrieved profile and the hygrometer soundings generally agree when their uncertainties are taken into account, although at 28 km and above the error bars from the two systems barely overlap. However, the profiles from the two systems behave differently with increasing altitude. Only one hygrometer operated above 20 km. It reported a constant 4 ppmv, while the retrieved mixing ratios grow monotonically with altitude above the 16 km level. The reason for this discrepancy is unknown. It is unlikely to be caused by the long response time of the hygrometer. According to estimates in Mastenbrook and Oltmans [1985], that effect would smooth the measurements over less than 0.5 km in the vertical. It could be due to the several hundred kilometer separation between the occultation and the hygrometer soundings. Large discrepancies seem to be the rule among stratospheric water vapor profiles measured simultaneously with different techniques. For example, Figures C-6 through C-8 of WMO [1985] illustrate the results of three intercomparison studies in which differences, both in magnitude and altitude dependence, among soundings by different techniques far exceed those presented here.

An increase in mixing ratio with altitude has also been noted recently in remote infrared experiments from balloons [e.g., Fischer et al., 1985] and in mid-latitude data [Russell et al., 1984] from the LIMS on the Nimbus-7 satellite. The altitude dependences exhibited by a large number of earlier observations, remote and in situ, are mixed [Elsaesser, 1983], but there is a tendency towards an increase in mixing ratio with height.

#### 4.3 Nitric Acid

Figure 8 presents the retrieved nitric-acid profile. Since we made no concurrent in-situ measurements of nitric acid, we show the "reasonableness" of the profile by superimposing it on a compilation [World Meteorological Organization, 1982] of profiles measured in previous years by other investigators. The data of Arnold et al. [1980] and Lazrus and Gandrud [1974] were obtained in situ, whereas all the other data were taken by remote infrared methods.

In common with the remote infrared data, our retrieved mixing ratio values are higher than those obtained in situ. However, in comparison with other infrared measurements they tend towards the low side. For example, Figure 9 shows a comparison between the retrieved profile and two independent measurements made on May 5, 1979, near Palestine, Texas. The first, obtained by the limb-emission technique, is from the Nimbus-7 LIMS [Gille et al., 1984]. The second measurement, intended as a correlative measurement for the LIMS observation, is from a balloon-based occultation experiment implemented with a filter radiometer [Fischer et al., 1985]. The peaks of all three profiles are located at nearly the same altitude, and the shapes of the profiles are similar. The maximum mixing ratio from our experiment is lower than those obtained from the others, but it should be noted that the differences are barely significant when the uncertainties of each experiment are taken into account. Near 31 km our profile lacks the secondary peak observed by Fischer et al.; otherwise those two profiles agree closely at levels above 25 km. The

profiles obtained by both occultation experiments fall off more rapidly above 25 km than does the LIMS profile. Furthermore, the LIMS profile falls off more rapidly than photochemical model predictions [Gille et al., 1984].

Figure 9 also shows the uncertainties in our retrieved nitric acid profile. They are approximately 10% at most levels, except at 14 and 32 km, where they are approximately 25%.

#### 4.4 CFC-12

Following Goldan et al. [1980], we plot the CFC-12 profiles against height above the tropopause. This minimizes apparent latitudinal and seasonal variations and facilitates comparisons among measurements. The retrieved CFC-12 profile, referenced to a tropopause height of 15 km, is shown in Figure 10. The profile extends only up to 22 km (which in the figure corresponds to 7 km above the tropopause). Absorption by CFC-12 is so weak that we get virtually no signal in observations at tangent heights above 22 km. The estimated uncertainties in the retrieved profile, indicated by the error bars, increase with altitude from under 10% at 12 km to 40% at 22 km. Along with the weakness of the atmospheric signal, the main causes of these large error bars are, first, the large uncertainty, estimated to be as high as 0.018, in the transmittances calculated for CFC-12 and, second, the effect of the overlapping absorption by nitric acid.

In a literature search for standards of comparison, we could not find any CFC-12 measurements, remote or in-situ, obtained since 1980 near 31°N latitude. Instead we show in Figure 10 an envelope of CFC-12 profiles based on the data in Figure 1-21 of the report by the World Meteorological Organization (WMO) [1982]. The WMO data, from the 40-45°N latitude band, are in-situ measurements originally made in the 1970's [Volz et al., 1981; Goldan et al., 1980] that were projected to 1981 to account for the expected increase in the CFC-12 abundance with time, roughly 5%/yr. Between 1981 and 1983 the same rate of increase was observed by Cunnold et al. [1986] in surface measurements at many locations. Assuming that the 5%/yr increase applied to the stratosphere as well as the surface, and that it continued beyond 1983, we used it to project the WMO data to 1985. The envelope of the twice-projected data is plotted in Figure 10, referenced to a tropopause height of 13 km [Goldan et al., 1980].

At all levels the retrieved mixing ratios agree with the projected values when the uncertainties in the retrieval are taken into account. However, above the tropopause the two barely overlap, and there is a distinct tendency for the retrieved values tend to be higher. It is known [e.g., Goldan et al., 1980] that CFC-12 lapse rates tend to decrease with decreasing latitude. Hence some of the difference may be caused by the difference in latitude between our measurement (31°N) and the WMO data (40-45°N). The minimum in the retrieved profile near the tropopause is of interest. It has a width in the vertical that is equal to or slightly larger than the approximately 3-km vertical resolution of the measurements and,

therefore, appears to be real. It is not very dependent on our correction for the overlapping absorption by nitric acid, since the structure survives when we remove or increase the correction. In addition, it is probably statistically significant, since the uncertainties in the profile are primarily systematic and are, therefore, correlated in the vertical. Assuming it is real, then, the structure may be related to the "folding" observed in some of the profiles of Goldan et al. [1980]. These authors suggest that folding is caused by an exchange of air between regions of different CFC-12 abundances.

## 5. CONCLUSION

From the third in our series of balloon-based infrared solar occultation experiments, performed with a non-scanning, multi-detector grating spectrometer, we retrieved mixing ratio profiles of ozone, water vapor, nitric acid, and CFC-12 between 12 and 35 km. The retrieved ozone and water vapor profiles were compared to concurrent data measured in-situ with ECC's and frost-point hygrometers. The nitric acid and CFC-12 profiles were compared with measurements in the literature. The objective has been to assess the feasibility of the technique for monitoring abundances of stratospheric constituents from operational satellites.

This experiment was more successful than our first one [Weinreb et al., 1984] for several reasons: The lower bounds of the measured profiles were extended down to 12 km, and this permitted detection of CFC-12. Also, the correlative in-situ measurements were of a higher quality. From the standpoint of obtaining successful retrievals, this experiment was also more successful than our second one. We have not reported the results from our second flight, because the measurements were affected by an unexpected feature, which we believe, but cannot prove, was an atmospheric absorption, possibly by aerosols from El Chichon. That feature prevented us from obtaining reasonable retrievals. If such a feature occurred commonly, it would diminish the utility of infrared limb measurements as a technique for monitoring the stratosphere, unless ways were found to remove its effect from the data.

In the experiment reported in this paper, the ozone results were clearly of a quality that would justify using the technique on operational satellites. The retrieved profile agreed well with concurrent ECC soundings at almost all altitudes. The largest disagreements, at altitudes below 25 km, averaged approximately 10%, which is also close to our estimate of the uncertainty in the retrieved ozone profile. The situation with water vapor was less clear. Typical of other infrared remote measurements of water vapor, the retrieved profile had relatively large uncertainties, which ranged between 10 and 30% in the stratosphere. The differences between the retrieved mixing ratios and the concurrent hygrometer data were smaller than the combined uncertainties of the measurements, but the altitude dependences of the profiles as measured by the two systems were different. Such disparities among simultaneously measured water profiles are, unfortunately, typical of other intercomparisons in the

literature.

The retrieved mixing-ratio profiles of nitric acid and CFC-12 were compared with previous measurements in the literature. (No concurrent in-situ measurements were made.) Nitric acid mixing ratios were consistent with the earlier data, particularly with those obtained by infrared limb techniques. The CFC-12 measurement is difficult to make, because with the moderate spectral resolution of this experiment the signal to noise ratio is low. Our measurement was compared with in-situ data obtained in the 1970's and projected to 1985 with a growth rate of 5%/yr. The retrieved mixing ratios were barely consistent with the projected data: below and at the tropopause the agreement was good, but the retrieved mixing ratios were higher than the projected data at the top of the profile. Although this experiment yielded profiles of nitric acid and CFC-12 that are reasonable, more experiments, preferably with coincident in-situ measurements, must be done before we can assess how successful the technique is for those gases.

#### ACKNOWLEDGMENTS

We are grateful for assistance from the following people: Lee D. Johnson, William A. Morgan, and Paige A. Bridges of NOAA/NESDIS for constructing the instrument and assisting in operating it; David G. Murcray and his group at the University of Denver for providing the gondola and the sun-seeker and making the flight arrangements; S. J. Oltmans of NOAA/ERL for making the ECC and frost-point hygrometer measurements; Walter R. Nagel and his group from NASA/Goddard Space Flight Center for providing the telemetry and data-recording system; A. Sanyal of the SM Systems and Research Corporation for the line-by-line transmittance calculations; Melvyn E. Gelman of the NOAA Climate Analysis Center for supplying the temperature and height profiles; Michael L. Hill of NOAA/NESDIS for assistance with the data handling; and Gene Dunlap and Frank Dutton of NOAA/NESDIS for photographing the figures. The balloon and helium were supplied by NASA through the auspices of Robert T. Watson. We thank the National Scientific Balloon Facility at Palestine for a smoothly run balloon launch and recovery.

## REFERENCES

- Arnold, F., R. Fabian, G. Henschen, and W. Joos, Stratospheric trace gas analysis from ions:  $H_2O$  and  $HNO_3$ , Planet. Space Sci., 28, 681-685, 1980.
- Chang, I-Lok and M. P. Weinreb, Data processing algorithms for inferring stratospheric gas concentrations from balloon-based solar occultation data. NOAA Tech. Rep. NESDIS 31, 29 pp., National Oceanic and Atmospheric Administration, U.S. Department of Commerce, Washington, DC, 1987.
- Cunnold, D. M., R. G. Prinn, R. A. Rasmussen, P. G. Simmonds, F. N. Alyea, C. A. Cardelino, A. J. Crawford, P. J. Fraser, and R. D. Rosen, Atmospheric lifetime and annual release estimates for  $CFCl_3$  and  $CF_2Cl_2$  from 5 years of ALE data, J. Geophys. Res., 91, 10,797-10,817, 1986.
- Ellesaesser, H. W., Stratospheric water vapor, J. Geophys. Res., 88, 3897-3906, 1983.
- Evans, W. F. J., H. Fast, J. B. Kerr, C. T. McElroy, R. S. O'Brien, D. I. Wardle, J. C. McConnell, and B. A. Ridley, Stratospheric constituent measurements from Project Stratoprobe, Proc. WMO Symposium on the Geophysical Aspects and Consequences of Change in the Composition of the Stratosphere, WMO Publ. 511, World Meteorological Organization, Geneva, 55-60, 1978.
- Farmer, C. B., O. F. Raper, B. D. Robbins, R. A. Toth, and C. Muller, Simultaneous spectroscopic measurements of stratospheric species:  $O_3$ ,  $CH_4$ ,  $CO$ ,  $CO_2$ ,  $N_2O$ ,  $H_2O$ ,  $HCl$ , and  $HF$  at northern and southern mid-latitudes, J. Geophys. Res., 85, 1621-1632, 1980.
- Fischer, H., F. Fergg, and D. Rabus, Radiometric measurements of stratospheric  $H_2O$ ,  $HNO_3$ , and  $NO_2$  profiles, Proc. International Radiation Symposium, Colorado State Univ., Fort Collins, 18-20, 1980.
- Fischer, H., F. Fergg, and D. Rabus, Stratospheric  $H_2O$  and  $HNO_3$  profiles derived from solar occultation measurements, J. Geophys. Res., 90, 3831-3843, 1985.
- Fontanella, J. C., A. Girard, L. Gramont, and N. Louisnard, Vertical distribution of  $NO$ ,  $NO_2$ , and  $HNO_3$  as derived from stratospheric absorption infrared spectra, Appl. Opt., 14, 825-839, 1975.
- Gille, J. C., P. L. Bailey, and J. M. Russell III, Temperature and composition measurements from the LRIR and LIMS experiments on Nimbus 6 and 7, Phil. Trans. R. Soc. London A, 296, 205-218, 1980.
- Gille, J. C., and J. M. Russell III, The Limb Infrared Monitor of the Stratosphere: experiment description, performance, and results, J. Geophys. Res., 89, 5125-5140, 1984.
- Gille, J. C., J. M. Russell III, P. L. Bailey, E. E. Remsberg, L. L. Gordley, W. F. J. Evans, H. Fischer, B. W. Gandrud, A. Girard, J. E. Harries, and S. A. Beck, Accuracy and precision of the nitric acid

concentrations determined by the Limb Infrared Monitor of the Stratosphere experiment on Nimbus 7, J. Geophys. Res., 89, 5179-5190, 1984.

Girard, A., J. Besson, L. Gramont, and E. Haziza, Spectrometre automatique aeroportee pour la surveillance des gaz a l'etat de trace dans la haute atmosphere, Meteorologie, 10, 3-14, 1977.

Goldan, P. D., W. C. Kuster, D. L. Albritton, and A. L. Schmeltekopf, Stratospheric  $\text{CFCl}_3$ ,  $\text{CF}_2\text{Cl}_2$ , and  $\text{N}_2\text{O}$  height profile measurements at several latitudes, J. Geophys. Res., 85, 413-423, 1980.

Goldman, A., F. S. Bonomo, and D. G. Murcray, Statistical-band-model analysis and integrated intensity for the 10.8  $\mu\text{m}$  band of  $\text{CF}_2\text{Cl}_2$ , Geophys. Res. Lett., 3, 309-312, 1976.

Goldman, A., F. S. Bonomo, F. P. J. Valero, D. Goorvitch, and R. W. Boese, Temperature dependence of  $\text{HNO}_3$  absorption in the 11.3- $\mu\text{m}$  region, Appl. Opt., 20, 172-175, 1981.

Harries, J. E., D. G. Moss, N. R. W. Swann, G. F. Neill, and P. Gildwarg, Simultaneous measurements of  $\text{H}_2\text{O}$ ,  $\text{NO}_2$ , and  $\text{HNO}_3$  in the daytime stratosphere from 15 to 35 km, Nature, 259, 300-302, 1976.

Harward, C. N., Pressure and temperature dependence of Freon-12 absorption coefficients for  $\text{CO}_2$  waveguide laser radiation, Appl. Opt., 17, 1018-1022, 1978.

Hilsenrath, E., W. Attmannspacher, A. Bass, W. Evans, R. Hagemeyer, R. A. Barnes, W. Komhyr, K. Mauersberger, J. Mentall, M. Proffitt, D. Robbins, S. Taylor, A. Torres, and E. Weinstock, Results from the balloon ozone intercomparison campaign (BOIC), J. Geophys. Res., 91, 13,137-13,152, 1986.

Kagann, R. H., J. W. Elkins, and R. L. Sams, Absolute band strengths of halocarbons F-11 and F-12 in the 8- to 16- $\mu\text{m}$  region, J. Geophys. Res., 88, 1427-1432, 1983.

Kent, G. S. and M. P. McCormick, SAGE and SAM II measurements of global stratospheric aerosol optical depth and mass loading, J. Geophys. Res., 89, 5303-5314, 1984.

Komhyr, W. D., Electrochemical concentration cells for gas analysis, Annals de Geophysique, 25, 203-210, 1969.

Krueger, A. J. and R. A. Minzner, A mid-latitude ozone model for the 1976 U. S. Standard Atmosphere, J. Geophys. Res., 81, 4477-4481, 1976.

Lazrus, A. L. and B. W. Gandrud, 1974: Distribution of stratospheric nitric acid vapor, J. Atmos. Sci., 31, 1102-1108, 1974.

Mastenbrook, H. J. and S. J. Oltmans, Stratospheric water vapor variability for Washington, DC/Boulder, CO: 1964-82, J. Atmos. Sci., 40, 2157-2165, 1983.

- McCormick, M. P., P. Hamill, T. J. Pepin, W. P. Chu, T. J. Swissler, and L. R. McMaster, Satellite studies of the stratospheric aerosol, Bull. Am. Meteor. Soc., 60, 1038-1046, 1979.
- McCormick, M. P., T. J. Swissler, E. Hilsenrath, A. J. Krueger, and M. T. Osborn, Satellite and correlative measurements of stratospheric ozone: comparison of measurements made by SAGE, ECC balloons, chemiluminescent, and optical rocketsondes, J. Geophys. Res., 89, 5315-5320, 1984.
- Murcray, D. G., A. Goldman, F. H. Murcray, F. J. Murcray, and W. J. Williams, Stratospheric distribution of  $\text{ClONO}_2$ , Geophys. Res. Lett., 6, 857-859, 1979.
- Murcray, D. G., F. H. Murcray, and W. J. Williams, A balloon-borne grating spectrometer, Appl. Opt., 6, 191-196, 1967.
- Remsberg, E. E., J. M. Russell III, J. C. Gille, L. L. Gordley, P. L. Bailey, W. G. Planet, and J. E. Harries, The validation of Nimbus 7 LIMS measurements of ozone, J. Geophys. Res., 89, 5161-5178, 1984.
- Rinsland, C. P., M. A. H. Smith, R. K. Seals, Jr., A. Goldman, F. J. Murcray, D. G. Murcray, J. C. Larsen, and P. L. Rarig, Stratospheric measurements of collision-induced absorption by molecular oxygen, J. Geophys. Res., 87, 3119-3122, 1982.
- Rodgers, C. D., R. L. Jones, and J. J. Barnett, Retrieval of temperature and composition from Nimbus 7 SAMS measurements, J. Geophys. Res., 89, 5280-5286, 1984.
- Rothman, L. S., R. R. Gamache, A. Barbe, A. Goldman, J. R. Gillis, L. R. Brown, R. A. Toth, J. -M. Flaud, and C. Camy-Peyret, AFGL atmospheric absorption line parameters compilation: 1982 edition, Appl. Opt., 22, 2247-2256, 1983.
- Russell, J. M. III, J. C. Gille, E. E. Remsberg, L. L. Gordley, P. L. Bailey, H. Fischer, A. Girard, S. R. Drayson, W. F. J. Evans, and J. E. Harries, Validation of water vapor results measured by the Limb Infrared Monitor of the Stratosphere experiment on Nimbus-7, J. Geophys. Res., 89, 5115-5124, 1984.
- Shaffer, W. A., J. H. Shaw, and C. B. Farmer, Effects of systematic errors on the mixing ratios of trace gases obtained from occultation spectra, Appl. Opt., 23, 2818-2826, 1984.
- Shapiro, M. M. and H. P. Gush, The collision-induced fundamental and first overtone bands of oxygen and nitrogen, Can. J. Phys., 44, 949-963, 1966.
- Smith, H. J. P., D. J. Dube, M. E. Gardner, S. A. Clough, F. X. Kneizys, and L. S. Rothman, FASCODE - fast atmospheric signature code (spectral transmittance and radiance). Rep. AFGL-TR-78-0081, 149 pp., Air Force Geophysics Lab., Bedford, MA, 1978.

Volz, A., U. Schmidt, J. Rudolph, D. H. Ehhalt, F. J. Johnson, and A. Khedim, Vertical profiles of trace gases at mid-latitudes, Berichte der Kernforschungsanlage Julich, Nr. 1742, FRG, 1981.

Weinreb, M. P., W. A. Morgan, I-Lok Chang, L. D. Johnson, P. A. Bridges, and A. C. Neuendorffer, High-altitude balloon test of satellite solar occultation instrument for monitoring stratospheric O<sub>3</sub>, H<sub>2</sub>O, and HNO<sub>3</sub>, J. Atmos. and Oceanic Tech., 1, 87-100, 1984.

World Meteorological Organization, The stratosphere 1981: theory and measurements, WMO Global Ozone Res. Monitoring Proj. Rep. No. 11, Geneva, 1982.

World Meteorological Organization, Atmospheric ozone 1985: assessment of our understanding of the processes controlling its present distribution and change, WMO Global Ozone Res. Monitoring Proj. Rep. No. 16, Geneva, 1985.

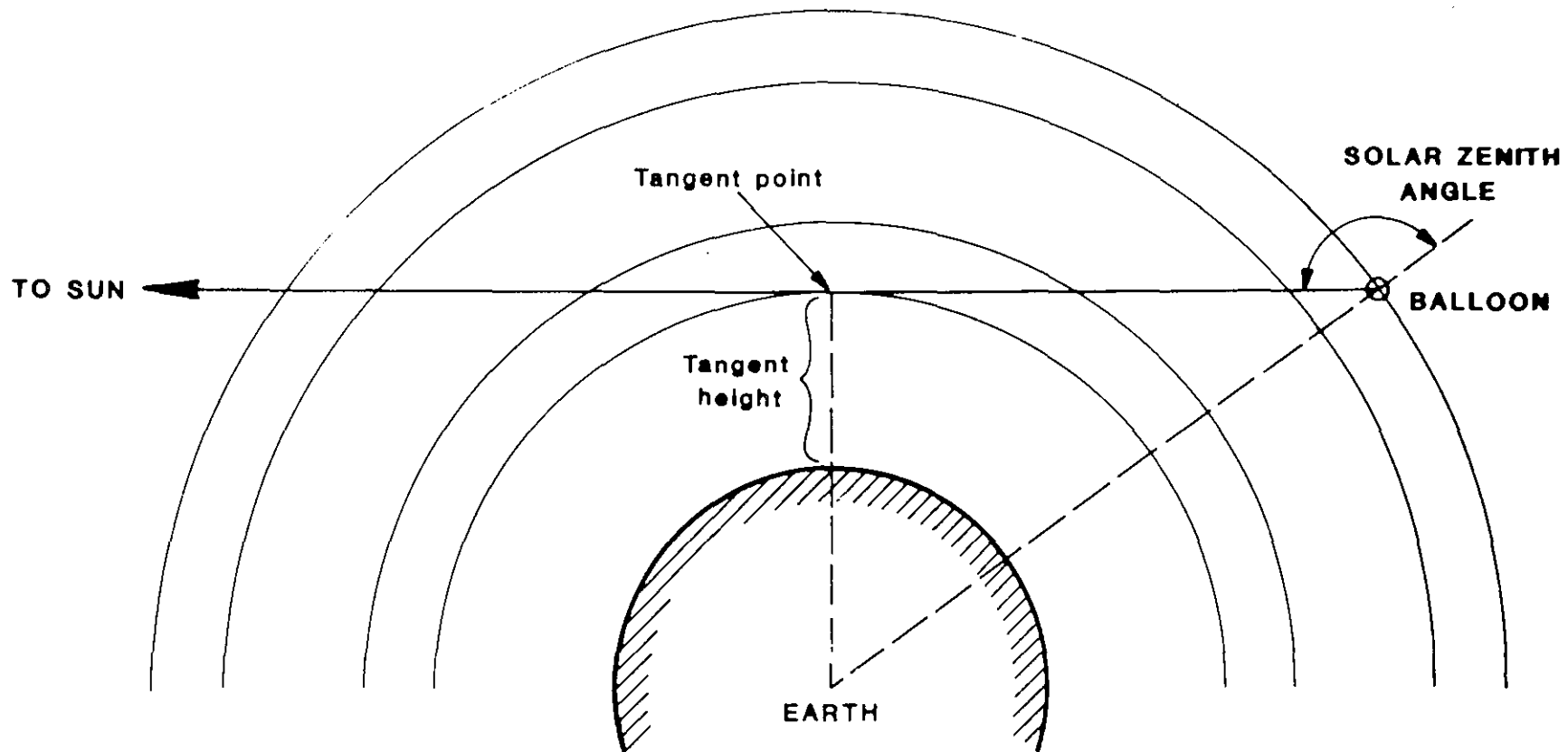


Figure 1. Solar occultation geometry, illustrating solar zenith angle, tangent point, and tangent height.

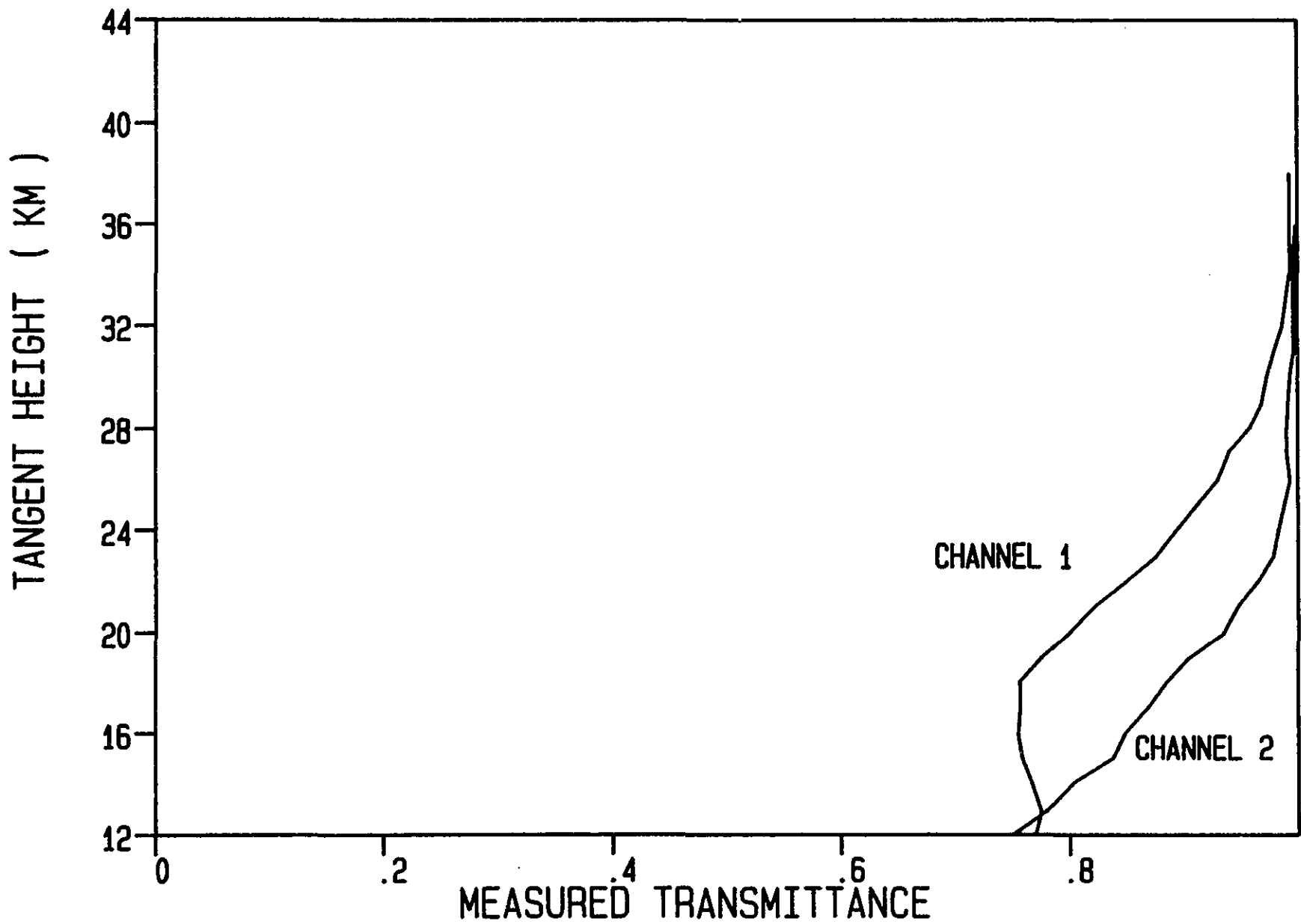


Figure 2. Measured transmittances in channel 1 (nitric acid) and channel 2 (CFC-12).

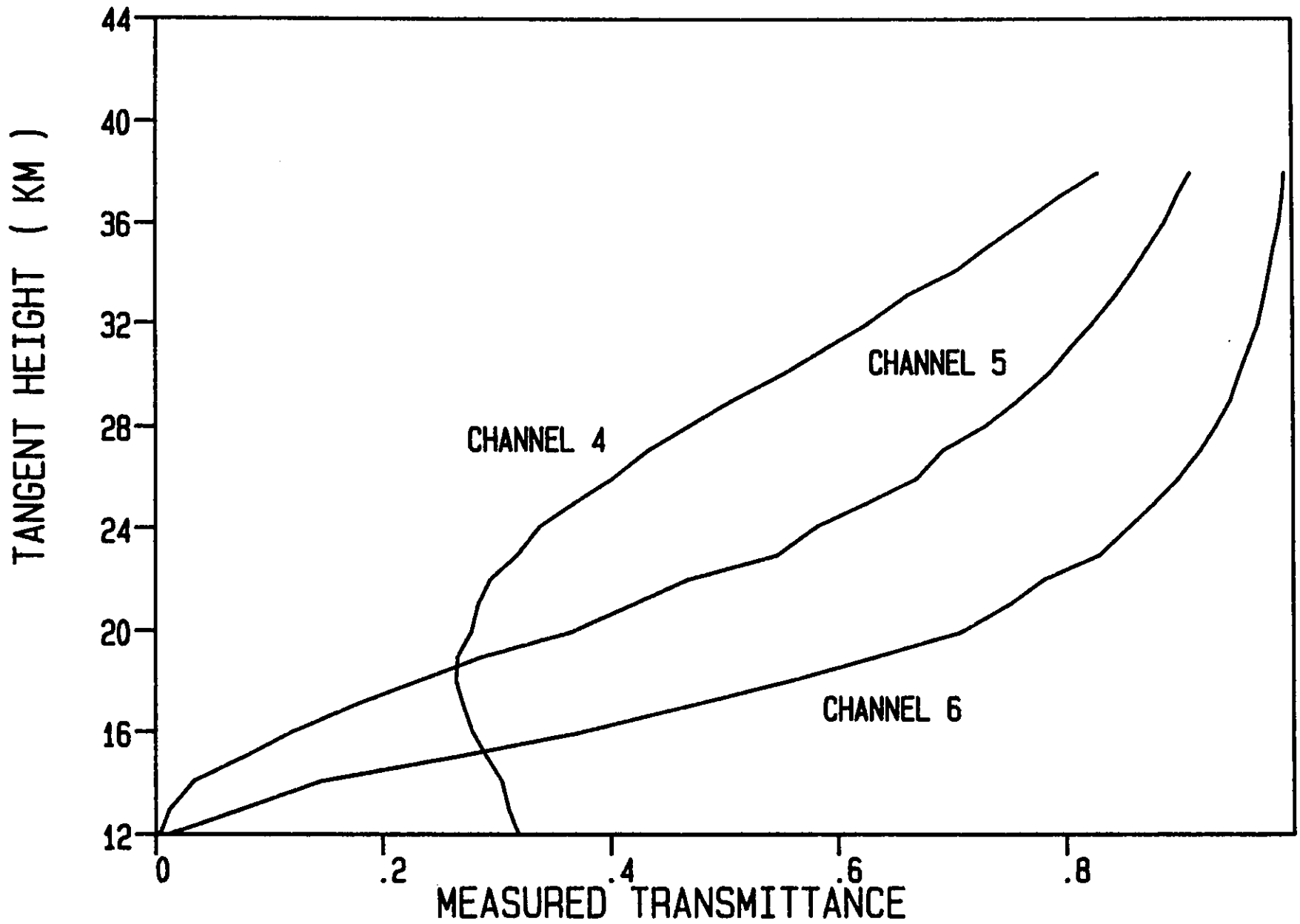


Figure 3. Measured transmittances in channel 4 (ozone) and channels 5 and 6 (water vapor).

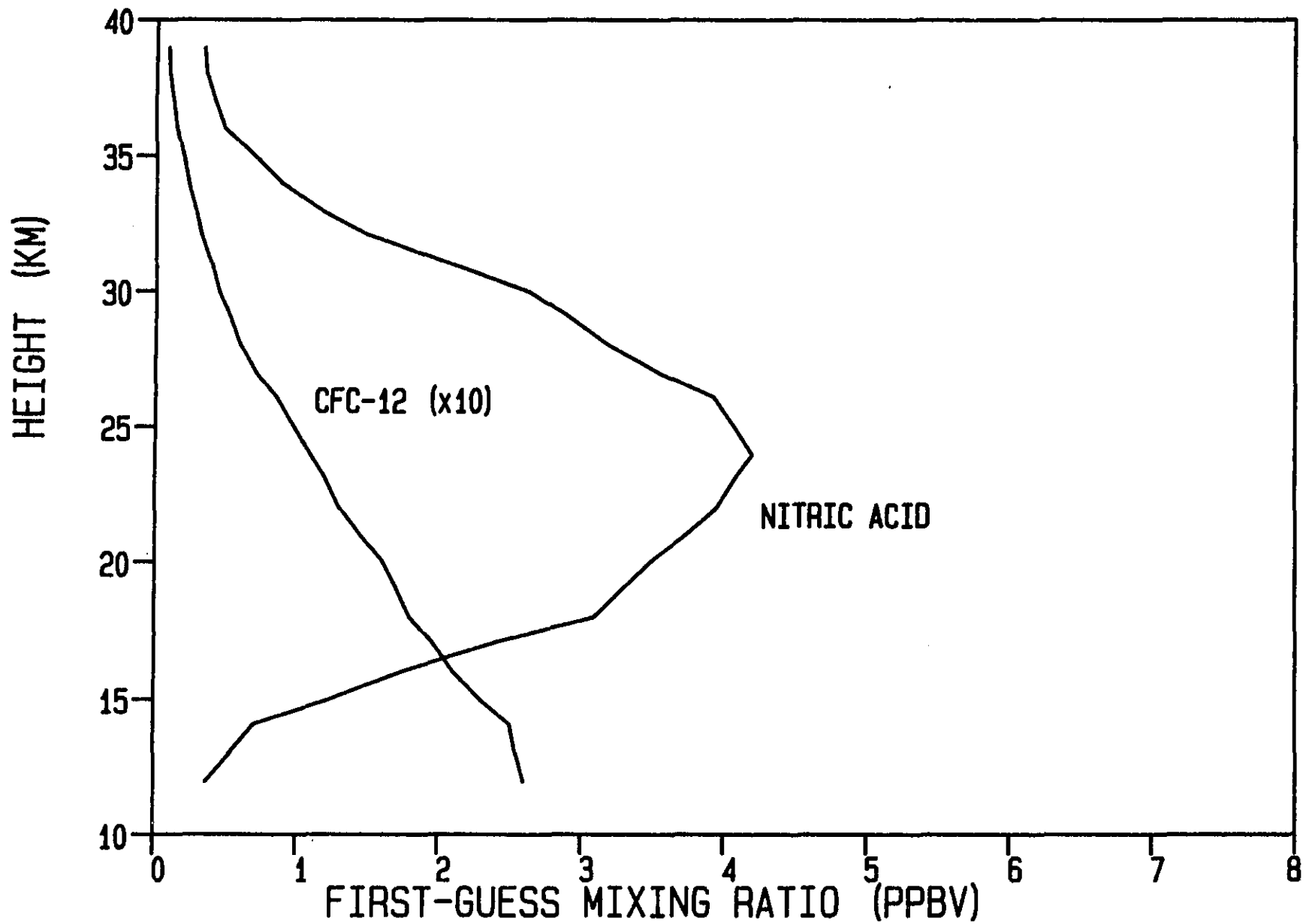


Figure 4. First-guess mixing ratio profiles for nitric acid and CFC-12. Note that CFC-12 values are multiplied by 10; e.g., mixing ratio at 24 km is 0.11 ppbv.

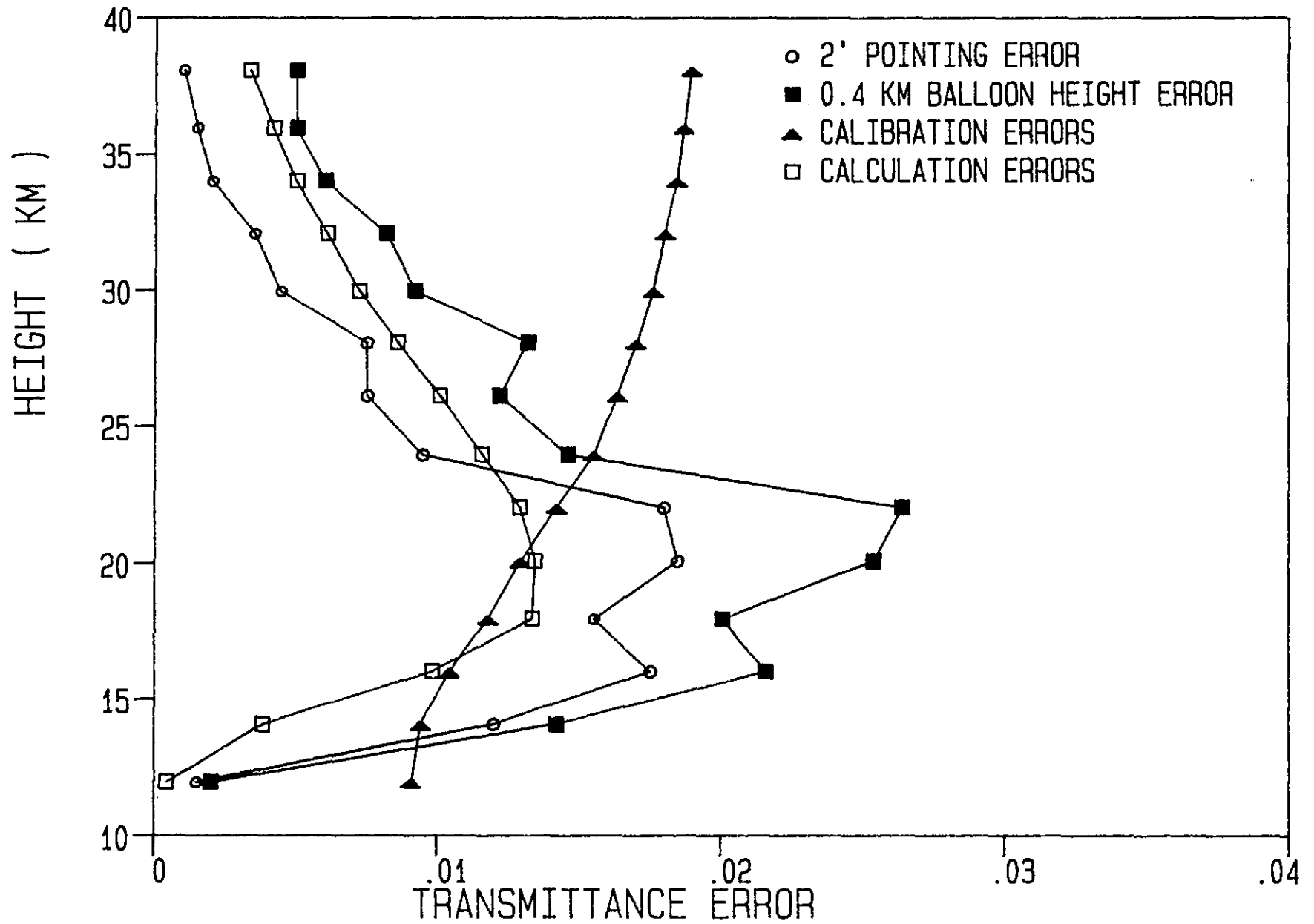


Figure 5. Estimated errors in transmittances for channel 5 for the four most important error sources. Note that the first three sources affect the measured transmittances, whereas the fourth is the estimated error in the calculated transmittances.

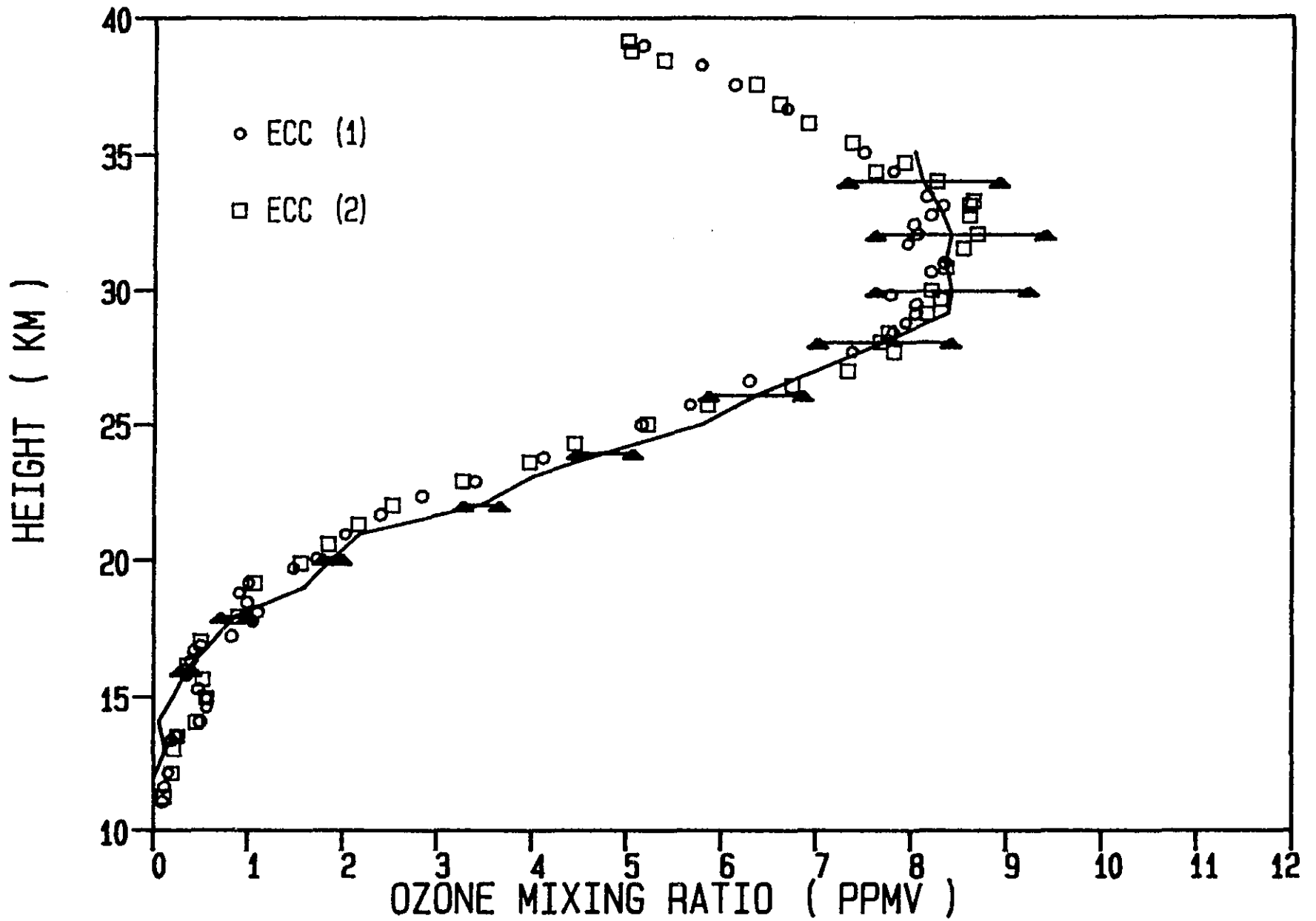


Figure 6. Retrieved ozone mixing ratio profile (curve with error bars) and concurrent ECC measurements.

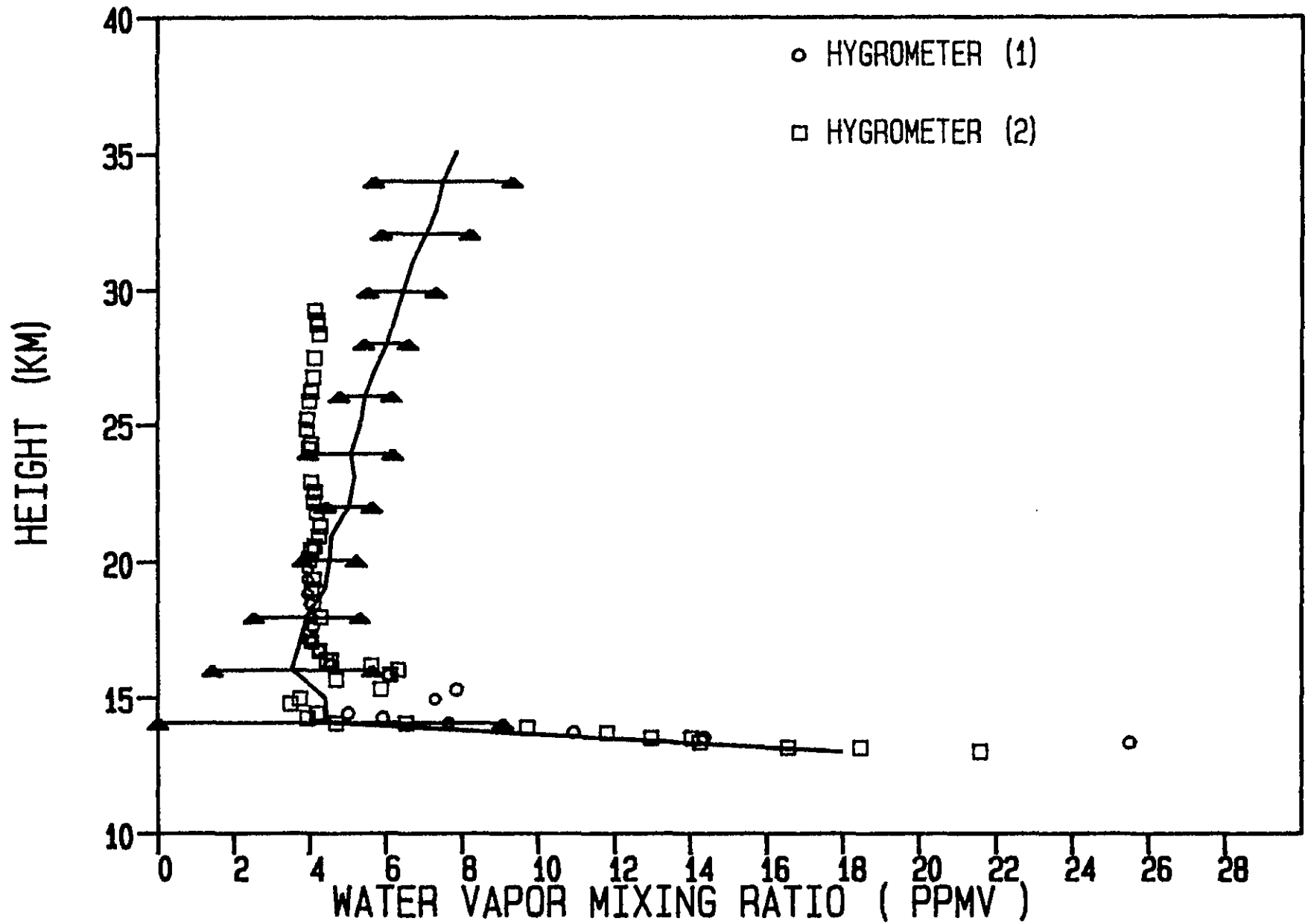


Figure 7. Retrieved water vapor mixing ratio profile (curve with error bars), and concurrent frost-point hygrometer measurements.

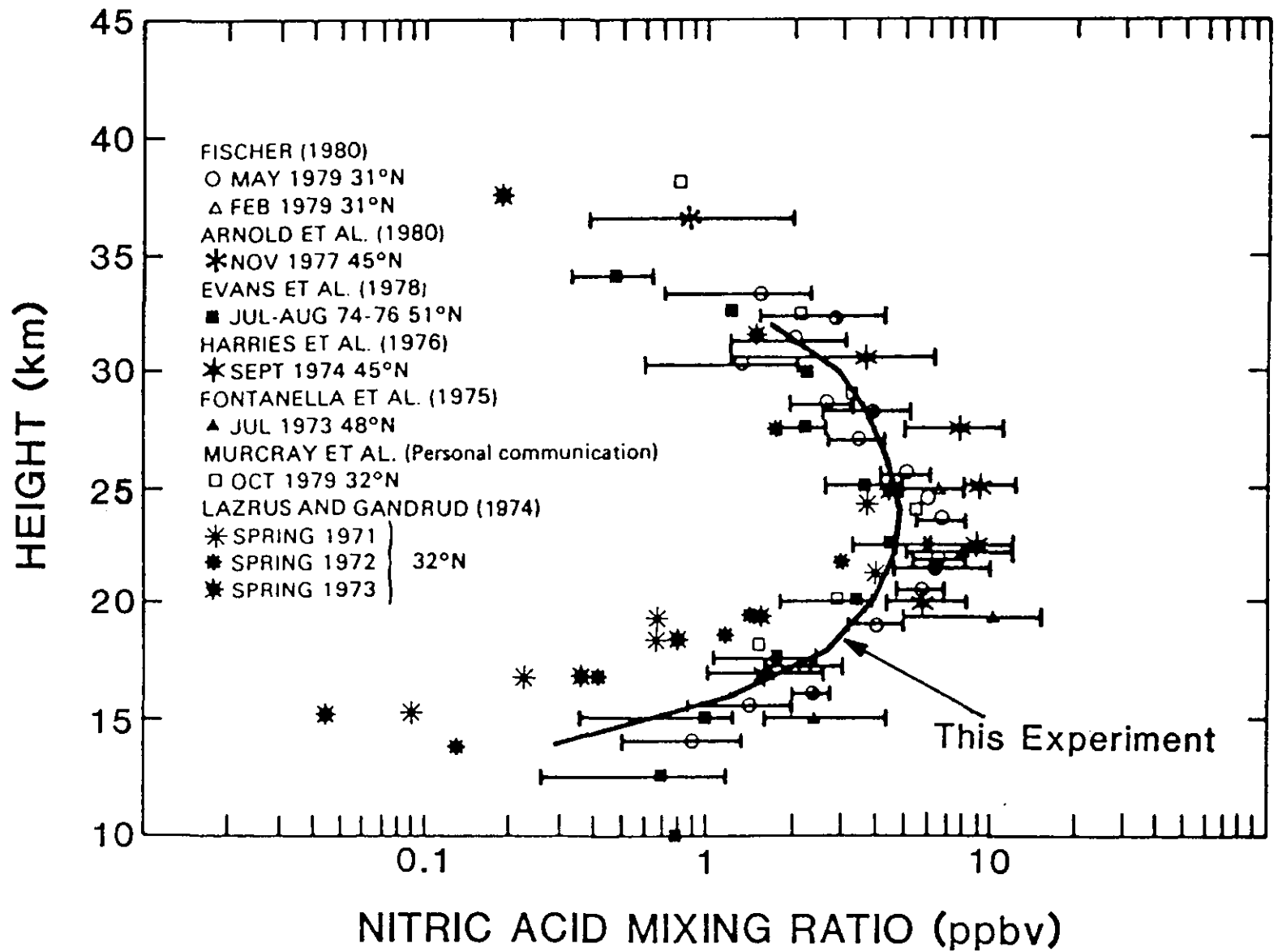


Figure 8. Retrieved nitric acid mixing ratio profile (solid curve) superimposed on compilation [WMO, 1982] of previous measurements.

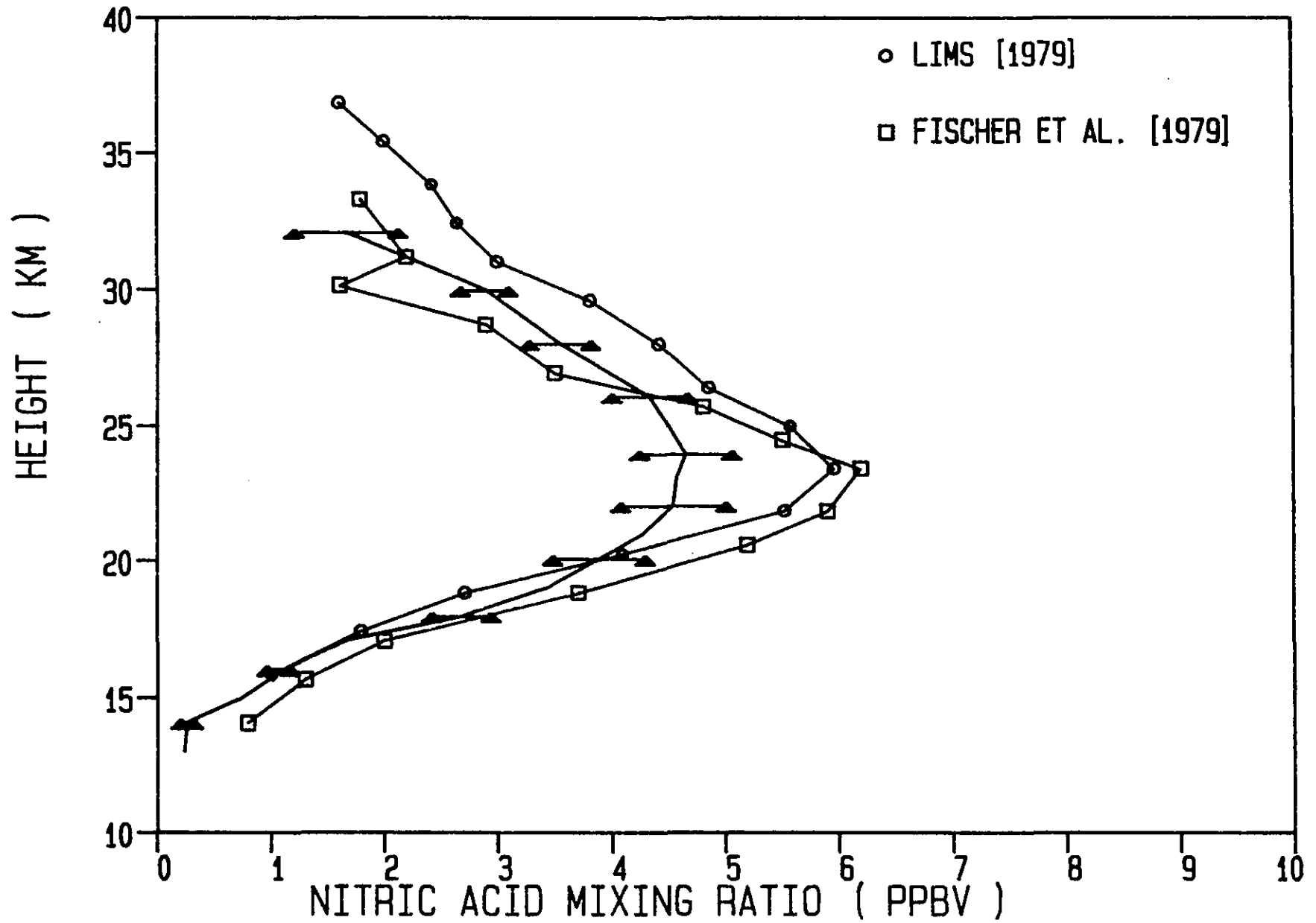


Figure 9. Retrieved nitric acid mixing ratio profile (curve with error bars), with two measurements made in 1979: LIMS [Gille et al., 1984] and occultation measurement of Fischer et al. [1985].

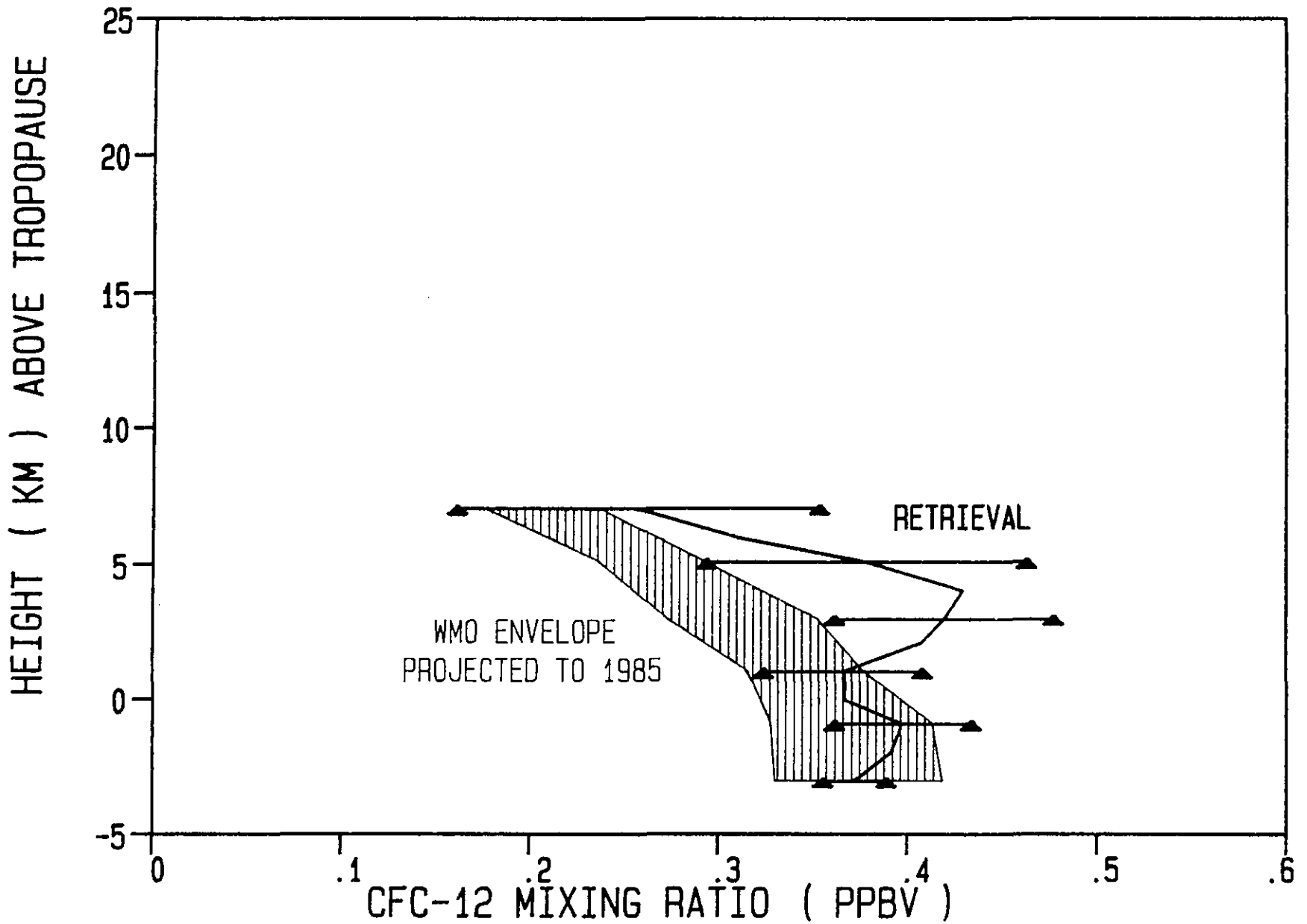


Figure 10. Retrieved CFC-12 mixing ratio profile (curve with error bars), with envelope of prior measurements [WMO, 1982] projected to 1985, assuming 5%/yr growth. Tropopause height is 15 km for the retrieved profile and 13 km for the prior measurements.